Journal of Magnetic Resonance 201 (2009) 93–99

Contents lists available at ScienceDirect

Journal of Magnetic Resonance

journal homepage: www.elsevier.com/locate/jmr

Magnetic resonance imaging of dissolved hyperpolarized ^{129}Xe using a membrane-based continuous flow system

N. Amor [a], P.P. Zänker [a], P. Blümler [a,b], F.M. Meise [c], L.M. Schreiber [c], A. Scholz [d], J. Schmiedeskamp [a], H.W. Spiess [a], K. Münnemann [a,c,*]

[a] Max Planck Institute for Polymer Research, Ackermannweg 10, 55128 Mainz, Germany
[b] Research Center Jülich, ICG Phytosphere, 52425 Jülich, Germany
[c] Section of Medical Physics, Department of Diagnostic and Interventional Radiology, Johannes Gutenberg University Medical Center Mainz, Langenbeckstr.1, 55131 Mainz, Germany
[d] Department of Anaesthesiology, Johannes Gutenberg University Medical Center Mainz, Langenbeckstr.1, 55131 Mainz, Germany

ARTICLE INFO

Article history:
Received 24 March 2009
Revised 11 August 2009
Available online 14 August 2009

Keywords:
Hyperpolarization
Xenon
NMR
MRI
Dissolution technique
Contrast agent

ABSTRACT

A technique for continuous production of solutions containing hyperpolarized ^{129}Xe is explored for MRI applications. The method is based on hollow fiber membranes which inhibit the formation of foams and bubbles. A systematic analysis of various carrier agents for hyperpolarized ^{129}Xe has been carried out, which are applicable as contrast agents for *in vivo* MRI. The image quality of different hyperpolarized Xe solutions is compared and MRI results obtained in a clinical as well as in a nonclinical MRI setting are provided. Moreover, we demonstrate the application of ^{129}Xe contrast agents produced with our dissolution method for lung MRI by imaging hyperpolarized ^{129}Xe that has been both dissolved in and outgassed from a carrier liquid in a lung phantom, illustrating its potential for the measurement of lung perfusion and ventilation.

1. Introduction

Hyperpolarized (HP) ^{129}Xe is increasingly applied for *in vivo* MRI (magnetic resonance imaging), e.g. in lung and brain imaging [1–6] and angiography [7]. The usage of HP noble gases (^{3}He, ^{129}Xe) is especially beneficial for lung MRI since conventional ^{1}H pulmonary MRI applications are limited by low sensitivity and contrast because of the low proton density in the lung. While inhaled HP ^{3}He is particularly well suited for ventilation measurements and depicting lung morphology [8–12], HP ^{129}Xe may be of great profit for perfusion measurements due to its higher solubility in liquids, e.g. blood [13]. Additionally, ^{129}Xe provides another important advantage: a large chemical shift difference of approx. 200 ppm between dissolved ^{129}Xe and gaseous ^{129}Xe can be observed. Xenon can pass the lung blood barrier, enabling perfusion and ventilation to be studied selectively and simultaneously. Hence, ^{129}Xe MRI can further elucidate the linkage of lung structure and function, identify cystic fibrosis, ventilation–perfusion mismatches of patients with pulmonary embolism, or monitor therapy of chronic obstructive pulmonary disease (COPD) [14]. In 2006, Driehuys et al. demonstrated the effectiveness of HP ^{129}Xe MRI for monitoring lung function by measuring the exchange of free xenon gas into the tissue and the red blood cells in the lung, providing a spatially resolved insight in alveolar–capillary gas transfer [15].

The dissolution of xenon into blood via inhalation is hindered by the presence of depolarizing oxygen and the slow passage into the cardiovascular system [13]. These problems can be circumvented by pre-dissolving xenon gas into a suitable carrier liquid and subsequent injection of this free diffusible, powerful MRI contrast agent [14,16]. The most important characteristics for the choice of ^{129}Xe carrier agents are (i) physiological tolerance of amounts in the order of milliliters for sufficient NMR signal, (ii) good xenon solubility, and (iii) a long ^{129}Xe T_1 relaxation time of the order of at least several tens of seconds. The last point is of particular importance since the hyperpolarization should be maintained as high as possible from the injection to the target tissue. Due to the strong lipophilic character of xenon, lipid emulsions naturally are good candidates as solvents, however, a drawback of this kind of carrier agents is their limited tolerance in the vascular system potentially causing thrombosis, embolism, and pulmonary edema when applied in high doses [7]. For saline solution, on the other hand, physiological compatibility of quantities from three to six times higher has been reported [17], but the xenon dissolution is limited due to its hydrophobic character. As plasma

* Corresponding author. Address: Max Planck Institute for Polymer Research, Ackermannweg 10, 55128 Mainz, Germany. Fax: +49 6131 379100.
E-mail address: muennemann@mpip-mainz.mpg.de (K. Münnemann).

1090-7807/$ - see front matter © 2009 Elsevier Inc. All rights reserved.
doi:10.1016/j.jmr.2009.08.004

expanders similarly have been designed to be applied in high rates, they might offer a good compromise between Xe solubility and physical tolerance.

The dissolution of xenon into a solvent is an important feature not only for *in vivo* MRI applications but also for many biological applications, such as the investigation of biomolecules or protein folding mechanisms [18–23], where methods such as 'shaking' or 'bubbling-and-stop' have been applied. Recently, the main obstacle of efficient and fast dissolution of HP ^{129}Xe without formation of foams or bubbles has been solved by applying a continuous flow system [24,25] on the basis of commercially available hollow fiber membranes, which are usually used for blood oxygenation as artificial lungs ("oxygenators") in heart–lung machines during cardiac surgery. The proof of concept for the membrane technique for the efficient dissolution of hyperpolarized Xe was demonstrated in Ref. [24] by ^{129}Xe NMR spectroscopy. At that time, a device was employed which continuously delivered hyperpolarized Xe to a stationary solvent but it was not capable of producing a continuous flow of Xe enriched liquid as it is necessary for *in vivo* MRI experiments.

In the present work, a commercially available membrane module has been used that provides a continuous flow of up to several tens of ml/min of the Xe enriched contrast agent and its usage for MRI applications has been explored. Adequate ^{129}Xe carrier agents are compared with regard to their NMR and MRI characteristics and the results of both spectroscopic and imaging experiments of HP ^{129}Xe are presented. Moreover, an application of the dissolution method for lung MRI is demonstrated, namely MRI of hyperpolarized ^{129}Xe gas outgassed from the carrier liquid in a lung phantom.

2. Materials and methods

2.1. NMR experimentals

Experiments were performed in a 4.72 T horizontal, 20 cm-bore solenoidal magnet (Magnex Scientific Ltd., UK) equipped with a Maran DRX spectrometer (Oxford Instruments, Oxfordshire, UK) and a 12 cm-bore gradient system (SGRAG 195/120/S, Magnex Scientific Ltd.) with maximal field gradient strength of 2.0 T/m/A ±5%. All images and spectra were acquired using a ^{1}H–^{129}Xe double resonance Litzcage coil (DSI-1200, Doty Scientific Inc., Columbia, USA) tuned to either the ^{129}Xe resonance frequency of 55.60 MHz or the ^{1}H resonance at 201.01 MHz, respectively. ^{129}Xe spectra were recorded in one scan with a rectangular 90° pulses (pulse length: 350 μs) during active solvent and xenon gas flow.

To demonstrate the capability of detecting dissolved hyperpolarized ^{129}Xe signals in a clinical setting, imaging experiments were performed in a 1.5 T full body scanner, type Magnetom Vision (Siemens Medical Solutions, Erlangen, Germany), with a ^{129}Xe resonance frequency of 17.56 MHz. The system is equipped with a broadband amplifier and a gradient system which is slightly stronger than in usual clinical scanners and enables a maximum gradient strength of 50 mT/m. Two different homebuilt coils were used for the imaging experiments. The first one was a solenoid coil with a diameter of 65 mm and a length of 120 mm which was built using a 2 mm copper wire with twelve windings, and shielded by a silver foil. The size of the coil is suitable for whole body imaging of small animals. Furthermore, a surface coil was built to obtain larger signal-to-noise ratios (SNR) of small objects. The coil had a diameter of 32 mm and consisted of five windings.

2.2. Xenonizer

The hyperpolarized (HP) ^{129}Xe was produced by spin-exchange optical pumping using an apparatus, built similarly to that reported in Ref. [26] at the Research Center Jülich. A gas mixture consisting of 4% xenon (natural isotope distribution), 9% N_2, and 87% ^{4}He at 7 bar was used for the hyperpolarization of ^{129}Xe. The degree of polarization that could be achieved was approximately 8%. The xenon polarizer was used in the continuous flow mode with a gas flow of 250 ml/min and the pressure of the gas mixture was reduced to 4 bar by a nonmagnetic needle valve before being fed into the xenonizer module. For the MRI experiments in the clinical scanner, the polarizer has been transported to the University Hospital Mainz and set up in the technical room next to the used tomograph.

The core part of the xenonizer [25] are hollow fiber oxygenator membranes made of polypropylene (CELGARD® X50, Membrana GmbH, Germany) commonly used in heart–lung machines and provide pore sizes of approximately 0.03 μm. The fibers are integrated into special modules that are commercially available (Mini Module, Membrane Contactors, Membrana GmbH, Germany). These modules were used to dissolve HP ^{129}Xe in various biocompatible solvents as depicted in Fig. 1.

Approx. 150 ml of solvent is circulated through the setup including the membrane module driven by a nonmagnetic pump at a rate of 5−7.5 ml/min. Simultaneously, HP ^{129}Xe counterflows through the membranes and dissolves into the liquid. After one passage through the membrane module, the xenon-enriched liquid can be removed and used for further applications.

2.3. Biocompatible carrier agents

Four different biocompatible liquids were analyzed with respect to their suitability to serve as Xe carrier agents. We investigated a lipid emulsion (Lipofundin® R 20% N, B. Braun Melsungen AG, Germany), commonly used for parenteral nutrition, consisting of soy oil (20%), egg lecithin (min. 75%), Glycerol (2.5%), α-Tocopheroland, and Natriumoleat. The second carrier was isotonic saline solution with a NaCl content of 0.9% (free flex®, Fresenius Kabi GmbH, Bad Homburg, Germany). Furthermore, two plasma expanders were tested as xenon carriers: the gelatine based Gelafundin (B. Braun Melsungen AG, Germany) which contains 4% gelatine polysuccinate, and the starch based Voluven® (Fresenius Kabi GmbH, Bad Homburg, Germany), which is composed from 6% Poly(*O*-2-hydroxyethyl-)starch, 0.9% NaCl, natriumhydroxide and hydrochloric acid. These liquids were systematically characterized and compared to each other with respect to chemical shifts and linewidths of the dissolved ^{129}Xe, the relative ^{129}Xe solubilities, and ^{129}Xe T_1 relaxation times.

Whereas the chemical shifts δ and the relative solubilities L could be determined from the positions and intensities of the signals in the spectrum, the SNR was not sufficient to determine T_1 from a series of acquisitions with small flip angles. Therefore, the following experiment was performed: The liquid was continuously circulated for 60 s and thereby thoroughly saturated with HP ^{129}Xe, before the membrane pump was stopped by a pneumatic valve controlled from the spectrometer and synchronized with the pulse sequence. After a defined, variable time τ, a FID signal (90°, single scan) was detected, reflecting the remaining signal intensity after exponential T_1 signal decay during the time τ. In order to reduce statistical errors, results of several T_1 measurements for each substance were averaged.

3. Results

3.1. Comparison of biocompatible carrier liquids

Fig. 2(C) shows a series of NMR spectra of hyperpolarized ^{129}Xe dissolved in different carrier liquids referenced to the free ^{129}Xe gas line of the sample (Fig. 2(A)). The sample consists of two tubes:

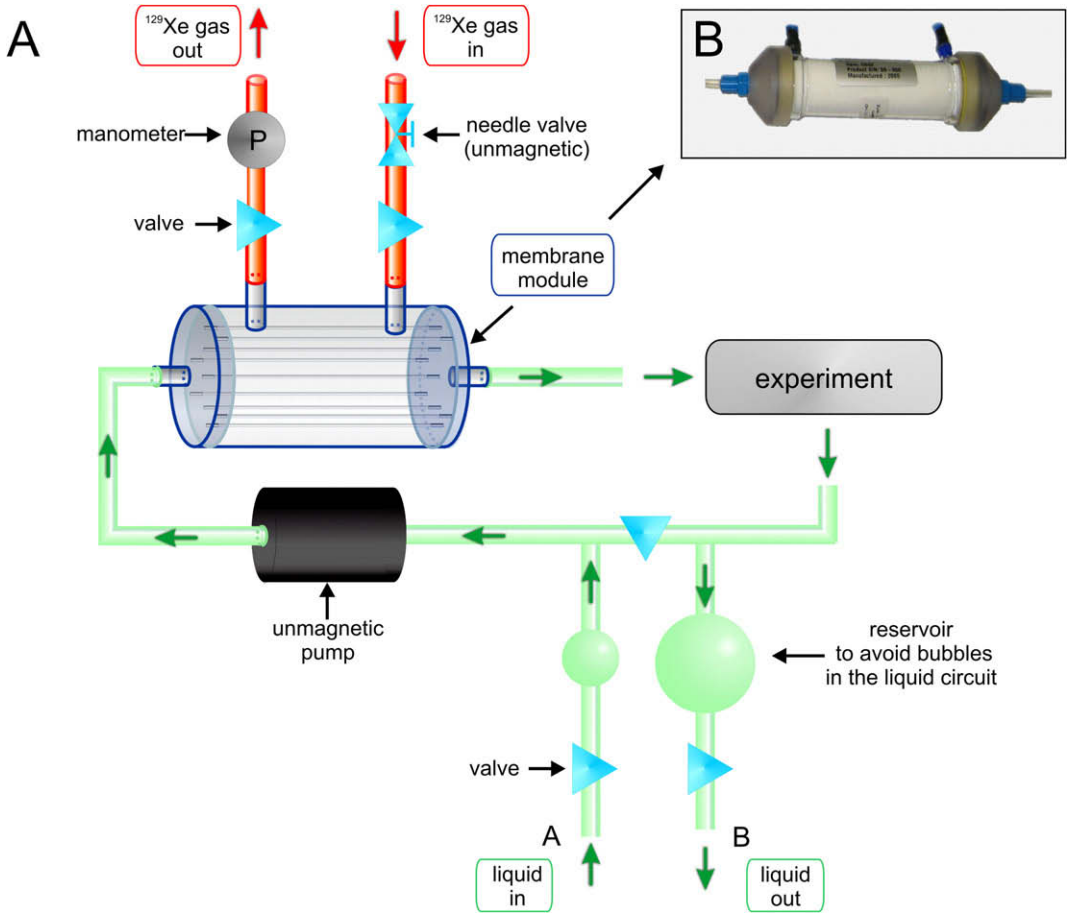

Fig. 1. (A) Principle xenonizer setup. (B) Photograph of a membrane module.

through the first one (indicated in green in Fig. 2(A), inner diameter 5.7 mm) the Xe enriched liquid is pumped and through the second one Xe gas (red in Fig. 2(A), inner diameter 2.6 mm). The spectrum of ^{129}Xe dissolved in Lipofundin® displays the highest signal intensity for the dissolved ^{129}Xe resonance (191–193 ppm) followed by the Voluven® solution. From the integral of the peaks of the dissolved ^{129}Xe, the relative ^{129}Xe solubilities in the liquids can be calculated and are given in Table 1 together with the respective chemical shifts and T_1 values.

The results for the T_1 relaxation times and chemical shifts for the saline and the fatty emulsion are in good agreement with literature [27]. Both plasma expanders show similar chemical shifts, good xenon solubilities, and long T_1 relaxation times of more than 1 min.

As examples for the image quality that can be obtained with these kinds of xenon-enriched liquids, Fig. 2(C) shows a number of FLASH (Fast Low Angle Shot) [28] projection images of tubes filled with the different solvents. The tubes were arranged in a loop through the RF coil and the Xe images were acquired during flow of the Xe enriched liquid as illustrated in Fig. 2(A). As reference, a Xe gas tube has also been placed inside the resonator. It appears shifted in the read direction due to its chemical shift (see Fig. 2(B)). The highest SNR in the ^{129}Xe images was obtained for Lipofundin® in the incoming tube, while the signal in the outgoing tube is decreased due to the higher number of RF pulses applied to the hyperpolarized ^{129}Xe during the second passage through the NMR coil as well as T_1 relaxation. As can be expected from comparison of the ^{129}Xe NMR spectra in Fig. 2(C), the images of the blood plasma expanders and the saline solution show smaller signal intensities than the Lipofundin® emulsion. The imaging results nicely reproduce the good xenon solubility of Lipofundin® as well as the long T_1 relaxation times in the plasma expanders demonstrated by the good SNR even in the back-flowing part of the loop, where the liquid arrives on the order of 30 s later.

3.2. Imaging of hyperpolarized ^{129}Xe in a clinical 1.5 T scanner

As the results in Section 3.1. suggest, Lipofundin® provides the best SNR for HP ^{129}Xe among the few tested and approved biocompatible carrier liquids. Therefore, it was used for MRI experiments in a clinical scanner using a solenoid coil with 65 mm diameter and 120 mm length. The T_1 relaxation time of the dissolved ^{129}Xe was measured also for this setup, as a field dependence of the relaxation was assumed in [14]. The T_1 relaxation time for Xe dissolved in Lipofundin at 1.5 T is 36 ± 7 s, which is slightly shorter than the obtained value at 4.7 T (43 ± 2 s, see Table 1) but nevertheless still sufficient for clinical applications. *In vitro* images of HP ^{129}Xe solutions were acquired to check the feasibility of the membrane dissolution method in real clinical applications. The results and a sketch of the phantom are shown in Fig. 3.

The phantom consists of two layers of PU (polyurethane) tubing (inner diameter = 4 mm), which are wound one over the other on a cylindrical support with an outer diameter of 50 mm (see Fig. 3(A)). The liquid is cycled from the membrane module through the phantom inside of the solenoid coil (setup shown in Fig. 1) while the image is acquired. Fig. 3(B) depicts a projection image of the phantom measured within an experiment time of 256 s; the obtained SNR is 24. The image clearly resembles the geometry of the phantom and demonstrates a good image quality. The outer part of the phantom, where the fresh hyperpolarized Xe solution

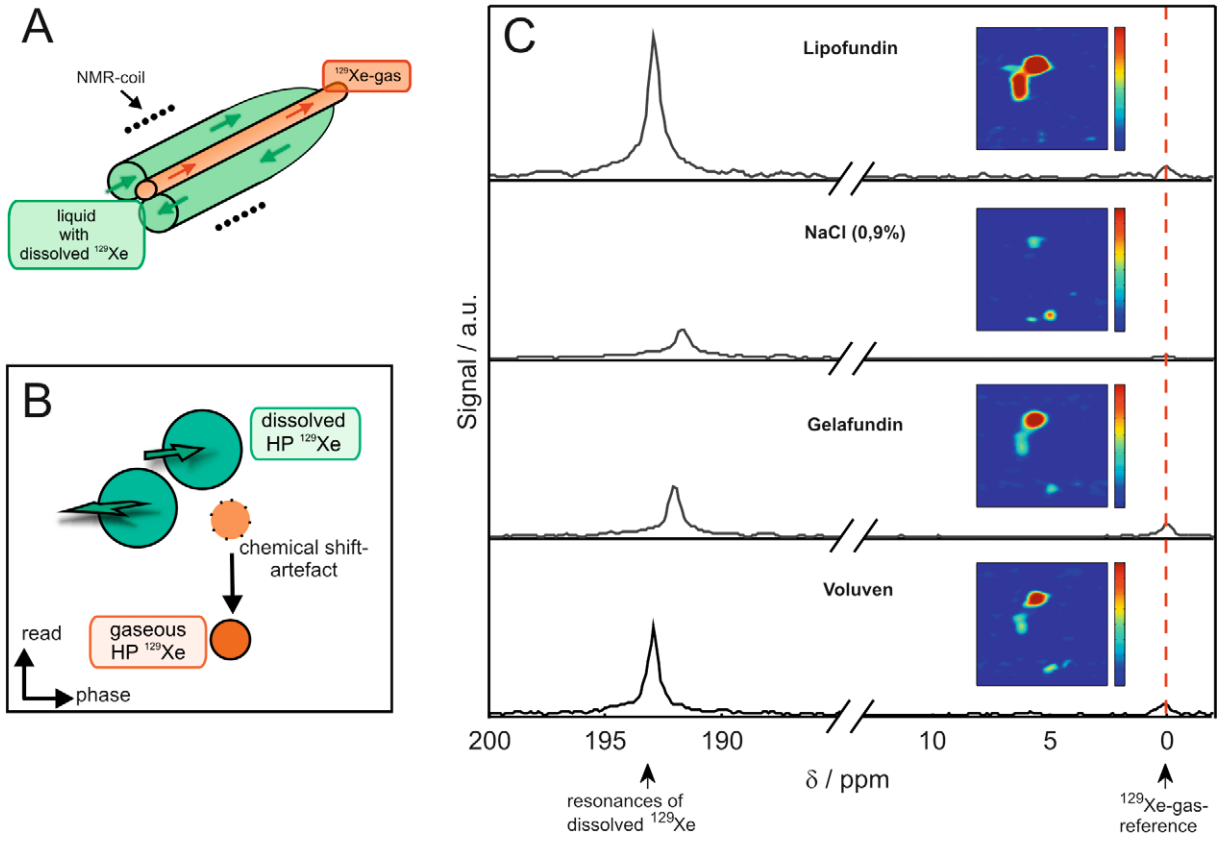

Fig. 2. (A) Sketch of the tube sample used for first spectroscopic and imaging experiments. The liquid tube (green) provides an inner diameter of 5.7 mm, the gas tube (red) an inner diameter of 2.6 mm. (B) Schematic view of expected MR images of axial 2D projections. (C) Xe NMR spectra (the red line denotes the chemical shift of Xe gas, which is used as an internal reference) and corresponding FLASH images of various flowing ^{129}Xe carrier liquids (TR = 0.5 s, TE = 1.5 ms, 4 Scans, flip angle: 90°, matrix size: (128 × 64) Px, FOV = (145 × 137) mm, only a region of interest is shown).

Table 1
^{129}Xe chemical shifts δ, line widths, solubilities L, and T_1 relaxation times of dissolved ^{129}Xe @ 4.7 T, errors indicate standard deviations from averages of multiple experiments.

Liquid	Chemical shift δ/ppm	Line width/ppm	Solubility $L/L_{\text{Lipofundin®}}$/%	Relaxation time T_1/s
Lipofundin®	193.0 ± 0.2	0.7	100	43 ± 2
NaCl (0.9%)	191.2 ± 0.3	0.9	21 ± 7	64.8 ± 1.2 [24]
Gelafundin	192.0 ± 0.1	0.8	36 ± 11	85.9 ± 5.0
Voluven®	192.3 ± 0.3	0.7	42 ± 16	78.9 ± 5.1

enters, shows a higher signal than the inner windings. This can be explained by the number of RF pulses, that have partly depolarized the hyperpolarized Xe solution on its way from the outer to the inner windings of the phantom.

Even images of very small amounts of liquid can be acquired in the clinical setting. For these experiments, a loop of the solvent bearing tube (inner diameter of 4 mm) was fed through a surface coil (32 mm diameter) in such a way that approximately two straight sections of the tube are in the active region of the coil (see Fig. 4(A)). The B_1 field of the coil excites only spins in a cylindrical volume with a diameter of 30 mm and a width of 20 mm. Consequently, only about 0.25 ml of liquid volume in each tube was excited. The liquid was cycled for about 10 s to dissolve HP ^{129}Xe, then the flow was stopped and the image was acquired. To increase the amount of xenon in the solution, a gas mixture with a fraction of 16% xenon was polarized. The image obtained by the FLASH

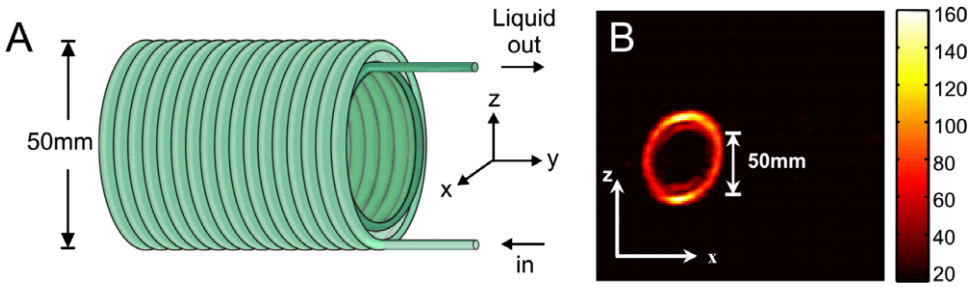

Fig. 3. (A) Sketch of phantom consisting of two layers of PU (polyurethane) tube which is flown through by HP ^{129}Xe dissolved in Lipofundin®. (B) Projection image of the phantom in the *xz*-plane. The image is acquired during liquid flow with a FLASH sequence and the following parameters: Flip angle: 45°, FOV: (200 × 200) mm, (64 × 64) Px, TR = 1 s, NS = 4.

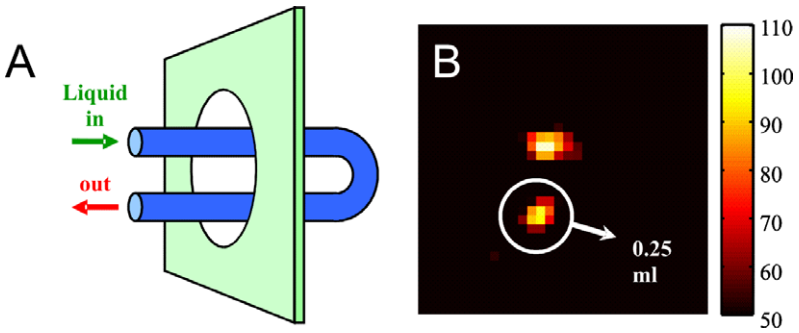

Fig. 4. (A) Sketch of imaging setup for small amounts of liquid. The green plane indicates the position of the surface coil. Only two narrow slices of the tubes are excited by the RF pulses. (B) Obtained FLASH image of the tubes filled with ^{129}Xe dissolved in Lipofundin® (stopped flow). Imaging parameters were: FOV (100 × 100) mm, (16 × 16) Px, TR = 100 ms, flip angle: 10°, NS = 2. (For interpretation of the references to color in this figure legend, the reader is referred to the web version of this paper.)

sequence in two scans is shown in Fig. 4. The two cross sections of the 4 mm tube which are excited by the surface coil are clearly visualized in the image. The obtained SNR for the image is 5.5.

3.3. MRI results of a lung phantom

A simplified lung phantom, represented by a second membrane module (M2), was introduced into the xenonizer setup (see Fig. 5). The setup mimics the passage of blood through the lung into which pre-dissolved HP ^{129}Xe has been injected. A minor pressure drop was applied at the membrane pump (50–100 mbar) in order to ensure a flow of ^{129}Xe outgassed from the carrier liquid through the sample. For MRI experiments, the sample consisted of two nested glass spheres: an inner sphere (diameter = 3 cm) filled with Lipofundin® with dissolved HP ^{129}Xe and an outer sphere (diameter = 6 cm) filled with HP ^{129}Xe outgassed from the carrier solvent in module M2 (schematically depicted in Fig. 5 as sample inside the NMR coil and in detail shown in Fig. 6(A) for comparison with imaging results). The glass sample was specifically built to have a clear spatial separation of gas and fluid space, yet having the dissolved and the ^{129}Xe outgassed from the liquid inside the resonator at the same time (as it would be the case for real lung measurements). By applying long and therefore chemically selective RF pulses, a selective excitation of either the dissolved or the outgassed ^{129}Xe was ensured. The ^{129}Xe gas T_1 relaxation time in the glass cell was determined to be approx. 120 s at 4 bar.

Experiments were performed using Lipofundin® as the ^{129}Xe carrier agent. Fig. 6 shows the results obtained in the glass sample filled with Xe solution and Xe gas after passage through the lung phantom.

While Fig. 6(A) depicts a sketch of the glass sample, images (B) and (C) provide reference images of the (outer) gas and the (inner) liquid space, acquired with HP ^{129}Xe directly from the polarizer and with ^{1}H in Lipofundin®, respectively, in order to provide an overview of the sample geometry. Fig. 6(D) presents an image of the HP ^{129}Xe gas outgassed from the lung phantom (M2) flowing through the outer part of the glass sample, while the degassed liquid was pumped through the inner part of the sample. The area where the Xe gas enters the glass phantom shows the highest signal, because the image was acquired by applying 90° pulses, which degrade the polarization during the passage of the phantom. An image of the liquid in this phantom, with excitation resonant on the dissolved ^{129}Xe frequency, showed no signal, demonstrating the degassing efficiency of the lung phantom module (M2).

4. Discussion

Our experiments demonstrate that the dissolution of xenon via membranes is an efficient method for the production of contrast agents enriched with hyperpolarized ^{129}Xe in a continuous flow

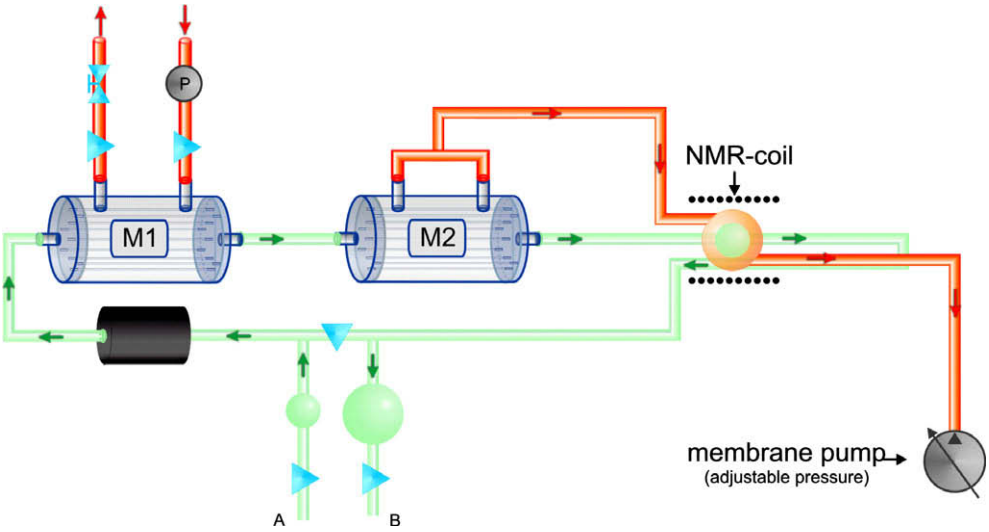

Fig. 5. Setup for lung phantom imaging experiments.

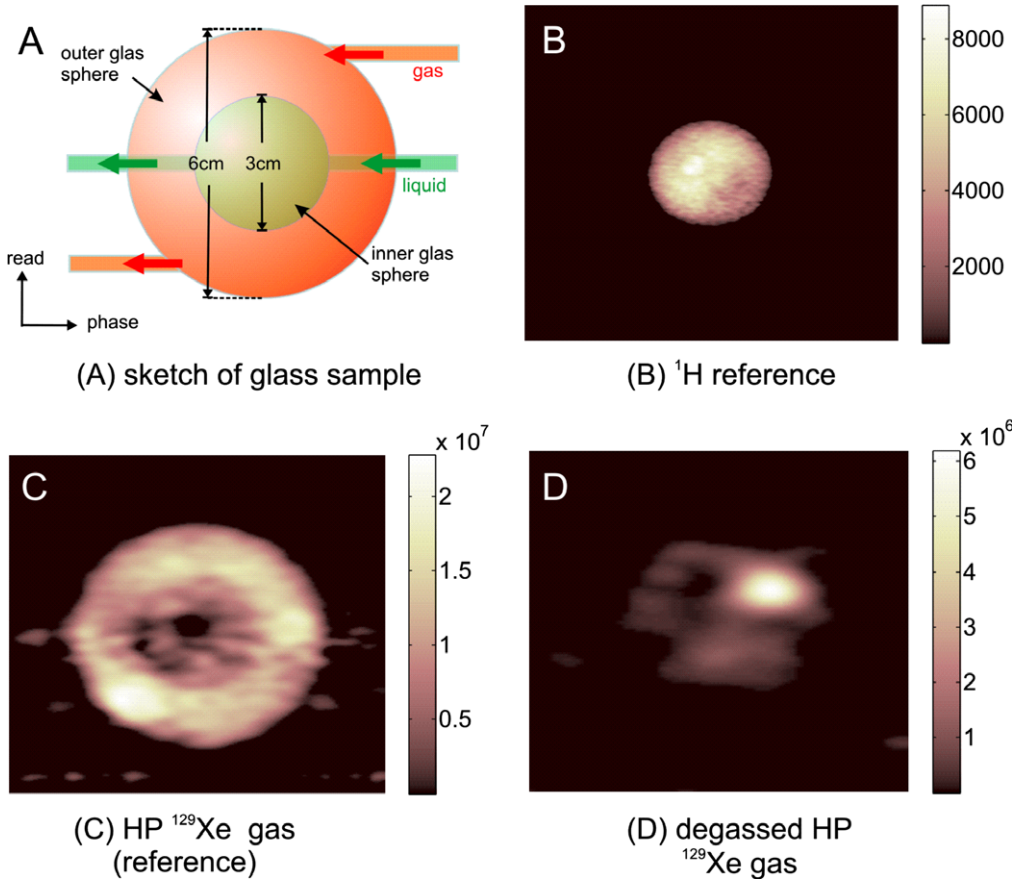

Fig. 6. ^{129}Xe MR images of glass sample. (A) Sketch of the used phantom (see also Fig. 5). (B–C) ^{1}H and ^{129}Xe reference images of solvent-filled inner and gas-filled outer sphere, respectively. For the acquisition of the gas reference, freshly hyperpolarized ^{129}Xe was led directly from the polarizer to the sample, without passing the membrane modules. (D) Image of HP ^{129}Xe that was outgassed from the carrier liquid in lung phantom module M2. (87 × 82) mm image sections of original (128 × 64) Px matrices shown. TR = 1 s. (B) Orginal FOV: (32 × 31) mm; 16 Scans. (C and D) Original FOV: (174 × 164) mm; 32 Scans. (B–D) Flip angle: 90°, TE = 1.5 ms).

mode. Comparison of the Xe gas signal intensities clearly shows that ^{129}Xe is not depolarized by passing the membranes in accordance with the results obtained in Ref. [24]. Thus, via this method, xenon can be directly dissolved without formation of foams or bubbles into suitable liquids for use as MRI contrast agents. The dissolution process is very fast and efficient: within seconds after switching on the pump the maximum signal amplitude is obtained [24]. Degassing of re-circulated liquid with a second module did not yield any increase in signal intensity, demonstrating the efficiency of the gas exchange in the membrane module.

Our analysis of biocompatible carrier agents (see Table 1) is in good agreement with the literature [14,27]. Although xenon dissolves best in the lipid emulsion, as expected from its lipophilic character, both plasma expanders also showed high Xe solubilities of 36% and 42%, respectively, and therefore also good MRI signal intensities. Even in saline solution, a sufficient amount of xenon could be dissolved in spite of its hydrophobic character via the membrane method to perform MRI experiments, however, the SNRs of these images are rather poor. From the MRI experiments, it can be concluded that Lipofundin®, Gelafundin, and Voluven® are suitable Xe carrier agents for *in vivo* MRI applications. Even the use of autologous blood or plasma as carrier liquid is possible since this is the original application of the oxygenator modules employed in this study. However, the choice of the optimal xenon carrier strongly depends on individual experimental parameters such as timing, required signal intensity, and physiological tolerance of the solvent.

For our MRI experiments in a clinical MRI setting, we chose Lipofundin® as the ^{129}Xe solvent, because it shows the highest solubility for xenon and sufficiently long T_1 relaxation time for the continuous flow measurements. In the imaging experiment performed on the clinical scanner (Fig. 3(B)), the two different layers of tubing are pictured nicely, the outer layer with a higher intensity, as the freshly polarized ^{129}Xe enters the phantom at this point. When the liquid arrives at the inner windings, it is already depolarized to a certain degree due to RF pulses. A good reproduction of sample structure is also shown in Fig. 4(B), proving that even small amounts of Xe carrying liquids (0.25 ml) can be detected. The imaged liquid volume is only one tenth of the amount of contrast agent which is usually employed in small animal studies (rats) without the danger to cause a fat embolism. Thus, similar *in vivo* MRI experiments should be feasible with the developed membrane method.

Experiments performed using the lung phantom (M2) showed that imaging experiments on Xe outgassed from the carrier liquid are possible despite the fast Xe relaxation in the liquid phase. In the MRI experiments (Fig. 6(B) and (C)), the reference images reproduce the sample structure very well, and Fig. 6(D) shows for the first time an image of ^{129}Xe outgassed from the carrier liquid. The entry area of the HPXe gas is over-emphasized because of 90° RF pulses which have been employed with short repetition times (TR) in order to minimize flow effects. Yet, the short TR inhibit the complete exchange of depolarized and hyperpolarized ^{129}Xe between acquisitions of subsequent k-space lines. Finally, a

shortened T_1 relaxation time inside the glass sample due to depolarization at the glass walls further reduced the image quality. This effect could effectively be minimized by special surface coatings [29,30]. The imaging experiments also prove the very efficient gas transport into and out of a solvent through the employed membranes modules. After the passage through the second membrane module the Xe outgassed from the carrier liquid could be easily detected whereas the lack of signal for the dissolved ^{129}Xe demonstrates the fast and efficient gas exchange in the lung phantom.

5. Conclusions

The new method of dissolving HP ^{129}Xe in various solvents via membranes has successfully been employed for MRI applications, featuring fast direct dissolution of Xe gas without formation of foams or bubbles, with good polarization retention, and the possibility of continuous operation even at high pressures. Several carrier agents for HP ^{129}Xe have been studied and compared. These results show that the most favorable solvent has to be chosen depending on the individual experimental requirements, i.e., weighting the solubility and thus the initial signal intensity against the ^{129}Xe T_1 relaxation time as well as the physiological tolerance of the carrier agent. Images acquired at high as well as at clinical magnetic field strengths were presented demonstrating the feasibility of the approach presented in this work for *in vivo* MRI applications. Hyperpolarized ^{129}Xe which was outgassed from the carrier liquid in a lung phantom has successfully been measured by MRI, indicating the possibility to apply pre-dissolved ^{129}Xe as a contrast agent in functional lung measurements.

Further improvement of imaging parameters will lead to better image quality and contrast, whereas investigations of new possible ^{129}Xe solvents, e.g. (clinical) PFC emulsions which will soon be commercially available, holds a potential for further improving ^{129}Xe NMR signal intensities and T_1 relaxation times, allowing for improved *in vivo* experiments in the near future.

Acknowledgements

We thank S. Appelt and W. Häsing (FZ Jülich) for the development of the xenon polarizer and H.-D. Lemke (Membrana GmbH) for the oxygenator fiber membranes. This work was supported by the "Kompetenznetz Asthma/COPD" (competence network for Asthma/COPD) funded by the Federal Ministry of Education and Research (FKZ01 GI 0868-0872) and the MAIFOR program of the Johannes Gutenberg University.

References

[1] W. Kilian, F. Seifert, H. Rinneberg, Dynamic NMR spectroscopy of hyperpolarized ^{129}Xe in human brain analyzed by an uptake model, Magn. Reson. Med. 51 (2004) 843–847.
[2] S. Patz, F. Hersman, I. Muradian, M. Hrovat, I. Ruset, S. Ketel, F. Jacobson, G. Topulos, H. Hatabu, J. Butler, Hyperpolarized ^{129}Xe MRI: a viable functional lung imaging modality?, Eur J. Rad. 64 (2007) 335–344.
[3] M.S. Albert, G.D. Cates, B. Driehuys, W. Happer, B. Saam, C.S. Springer Jr., A. Wishnia, Biological magnetic resonance imaging using laser-polarized ^{129}Xe, Nature 370 (1994) 199–201.
[4] B.M. Goodson, Y.-Q. Song, R.E. Taylor, V.D. Schepkin, K.M. Brennan, G.C. Chingas, T.F. Budinger, G. Navon, A. Pines, *In vivo* NMR and MRI using injection delivery of laser-polarized xenon, Proc. Natl. Acad. Sci. 94 (1997) 14725–14729.
[5] J.P. Mugler III, B. Driehuys, J.R. Brookeman, G.D. Cates, S.S. Berr, R.G. Bryant, T.M. Daniel, E.E. de Lange, J.H. Downs III, C.J. Erickson, W. Happer, D.P. Hinton, N.F. Kassel, T. Maier, C.D. Phillips, B.T. Saam, K.L. Sauer, M.E. Wagshul, MR imaging and spectroscopy using hyperpolarized ^{129}Xe gas: preliminary human results, Magn. Reson. Med. 37 (1997) 809–815.
[6] S.D. Swanson, M.S. Rosen, B.W. Agranoff, K.P. Coulter, R.C. Welsh, T.E. Chupp, Brain MRI with laser-polarized ^{129}Xe, Magn. Reson. Med. 38 (1997) 695–698.
[7] H.E. Möller, M.S. Chawla, X.J. Chen, B. Driehuys, L.W. Hedlund, C.T. Wheeler, G.A. Johnson, Magnetic resonance angiography with hyperpolarized ^{129}Xe dissolved in a lipid emulsion, Magn. Reson. Med. 41 (1999) 1058–1064.
[8] E.J.R. van Beek, J.M. Wild, H.-U. Kauczor, W. Schreiber, J.P. Mugler III, E.E. de Lange, Functional MRI of the lung using hyperpolarized 3-helium gas, J. Magn. Reson. 20 (2004) 540–554.
[9] A.J. Deninger, B. Eberle, M. Ebert, T. Großmann, W. Heil, H.-U. Kauczor, L. Lauer, K. Markstaller, E. Otten, J. Schmiedeskamp, W. Schreiber, R. Surkau, M. Thelen, N. Weiler, Quantification of regional intrapulmonary oxygen partial pressure evolution during apnea by ^{3}He MRI, J. Magn. Reson. 141 (1999) 207–216.
[10] K.K. Gast, K. Hawig, M. Windirsch, K. Markstaller, W.G. Schreiber, J. Schmiedeskamp, C. Düber, H.U. Kauczor, C.P. Heussel, Intrapulmonary ^{3}He gas distribution depending on bolus size and temporal bolus placement, Invest. Radiol. 43 (2008) 439–446.
[11] K.K. Gast, A. Biedermann, A. Herweling, W.G. Schreiber, J. Schmiedeskamp, E. Mayer, C.P. Heussel, K. Markstaller, H.U. Kauczor, B. Eberle, Oxygen-sensitive He-3-MRI in bronchiolitis obliterans after lung transplantation, Eur. Radiol. 18 (2008) 530–537.
[12] R.H. Acosta, P. Blümler, L. Agulles-Pedros, A.E. Morbach, J. Schmiedeskamp, A. Herweling, U. Wolf, A. Scholz, W.G. Schreiber, W. Heil, M. Thelen, H.W. Spiess, Controlling diffusion of ^{3}He by buffer gases: structural contrast agent in lung MRI, J. Magn. Reson. Imaging 24 (2006) 1291–1297.
[13] A. Bifone, Y.-Q. Song, R. Seydoux, R.E. Taylor, B.M. Goodson, T. Pietrass, T.F. Budinger, G. Navon, A. Pines, NMR of laser-polarized xenon in human blood, Proc. Natl. Acad. Sci. USA 93 (1996) 12932–12936.
[14] B.M. Goodson, Advances in magnetic resonance, nuclear magnetic resonance of laser-polarized noble gases in molecules, materials, and organisms, J. Magn. Reson. 155 (2002) 157–216.
[15] B. Driehuys, G.P. Cofer, J. Pollaro, J.B. Mackel, L.W. Hedlund, G.A. Johnson, Imaging alveolar–capillary gas transfer using hyperpolarized ^{129}Xe MRI, PNAS 103 (2006) 18278–18283.
[16] G. Duhamel, P. Choquet, E. Grillon, L. Lamalle, J.-L. Leviel, A. Ziegler, A. Constantinesco, Xenon-129 MR imaging and spectroscopy of rat brain using arterial delivery of hyperpolarized xenon in a lipid emulsion, Magn. Reson. Med. 46 (2001) 208–212.
[17] D. Morton, J.A. Safron, D.W. Rice, D.M. Wilson, R.D. White, Effects of infusion rates in rats receiving repeated large volumes of saline solution intravenously, J. Lab. Animal Sci. 47 (1997) 656–659.
[18] R.F. Tilton, I.D. Kuntz, Nuclear magnetic resonance studies of xenon-129 with myoglobin and hemoglobin, Biochemistry 21 (1982) 6850–6857.
[19] S.M. Rubin, M.M. Spence, I.E. Dimitrov, E.J. Ruiz, A. Pines, D.E. Wemmer, Detection of a conformational change in maltose binding protein by ^{129}Xe NMR spectroscopy, J. Am. Chem. Soc. 123 (2000) 8616–8617.
[20] M.M. Spence, S.M. Rubin, I.E. Dimitrov, E.J. Ruiz, D.E. Wemmer, A. Pines, S.Q. Yao, F. Tian, P.G. Schultz, Functionalized xenon as a biosensor, Proc. Natl. Acad. Sci. USA 98 (2001) 10654–10657.
[21] S. Han, S. Garcia, T.J. Lowery, E.J. Ruiz, J.A. Seeley, L. Chavez, D.S. King, D.E. Wemmer, A. Pines, Improved NMR based bio-sensing with optimized delivery of polarized ^{129}Xe to solutions, Anal. Chem. 77 (2005) 4008–4012.
[22] L. Schröder, T.J. Lowery, C. Hilty, D.E. Wemmer, A. Pines, Molecular imaging using a targeted magnetic resonance hyperpolarized biosensor, Science 314 (2006) 446–449.
[23] P. Berthault, A. Bogaert-Buchmann, H. Desveaux, G. Huber, Y. Boulard, Sensitivity and multiplexing capabilities of MRI based on polarized Xe biosensors, J. Am. Chem. Soc. 130 (2008) 16456–16457.
[24] D. Baumer, E. Brunner, P. Blümler, P.P. Zänker, H.W. Spiess, NMR spectroscopy of laser-polarised ^{129}Xe under continuous flow. A method to study aqueous solutions of biomolecules, Angew. Chem. Intern. Ed. 45 (2006) 7282–7284.
[25] P. Blümler, H.-D. Lemke, D. Krieter, H.-W. Spiess, F. Wiese, P.-P. Zänker, Patent application DE102005026604A1, Disclosed 14.12.2006.
[26] N.J. Shah, T. Ünlü, H.-P. Wegener, H. Halling, K. Zilles, S. Appelt, Measurement of rubidium and xenon absolute polarization at high temperatures as a means of improved production of hyperpolarized ^{129}Xe, NMR Biomed. 13 (2000) 214–219.
[27] A.K. Venkatesh, L. Zhao, D. Balamore, F.A. Jolesz, M.S. Albert, Evaluation of carrier agents for hyperpolarized xenon MRI, NMR Biomed. 13 (2000) 245–252.
[28] A. Haase, J. Frahm, D. Matthaei, W. Haenicke, K.-D. Merboldt, FLASH imaging, rapid NMR imaging using low flipangle pulses, J. Magn. Reson. 67 (1986) 258–266.
[29] S.R. Breeze, S. Lang, I. Moudrakovski, C.I. Ratcliffe, J.A. Ripmeester, B. Simard, Coatings for optical pumping cells and extending the lifetime of hyperpolarized xenon, J. Appl. Phys. 86 (1999) 4040–4042.
[30] I.L. Moudrakovski, S.R. Breeze, B. Simard, C.I. Ratcliffe, J.A. Ripmeester, T. Seideman, J.S. Tse, G. Santyr, I. Zuger, Coatings for optical pumping cells and short-term storage of hyperpolarized xenon, J. Chem. Phys. 114 (2001) 4040–4042.